IEIE Transactions on Smart Processing and Computing, vol. 5, no. 6, December 2016
https://doi.org/10.5573/IEIESPC.2016.5.6.440

Near-field Noise-emission Modeling for Monitoring Multimedia Operations in Mobile Devices

Eakhwan Song[1], Jieun Choi[2], and Young-Jun Lee[2]

[1] Department of Electronics and Communications Engineering, Kwangwoon University / Seoul, Korea esong@kw.ac.kr
[2] National Security Research Institute / Daejeon, Korea {choije,lhyjlee}@nsr.re.kr

***** Corresponding Author: Eakhwan Song

Received December 6, 2016; Revised December 12, 2016; Accepted December 13, 2016; Published December 30, 2016

** Short Paper*

***Abstract*:** In this paper, an equivalent circuit model for near-field noise emission is proposed to implement a multimedia operation–monitoring system for mobile devices. The proposed model includes a magnetic field probe that captures noise emissions from multimedia components, and a transfer function for near-field noise coupling from a transmission line source to a magnetic field probe. The proposed model was empirically verified with transfer function measurements of near-field noise emissions from 10 kHz to 500 MHz. With the proposed model, a magnetic field probe was optimally designed for noise measurement on a camera module and an audio codec in a mobile device. It was demonstrated that the probe successfully captured the near-field noise emissions, depending on the operating conditions of the multimedia components, with enhanced sensitivity from a conventional reference probe.

***Keywords*:** Near-field noise, Magnetic probe, Multimedia operation monitoring

1. Introduction

In recent years, mobile devices have enabled not only wireless communications but also a variety of multimedia functionality, including audio, video, and even virtual reality. Associated with a drastic increase in communications throughput, which has allowed large-scale data transmission, multimedia functions have become one of the most significant features of mobile devices [1]. Fig. 1 depicts a camera module and an audio codec component integrated in a modern wireless mobile device. In most cases, multimedia functions in mobile devices are employed for entertainment; meanwhile, the significantly evolved capacity for recording and playing multimedia content can be abused for illegal purposes, including unauthorized voice recordings and hidden filming.

In the industry, various products and technical white papers regarding the theory of detecting illegal multimedia abuses have been introduced. Most of the approaches capture the electromagnetic noise emissions of multimedia components from a long physical range depending on their operating conditions [2]. However, electromagnetic emissions from the components are mitigated by using shielding and grounding techniques to reduce the

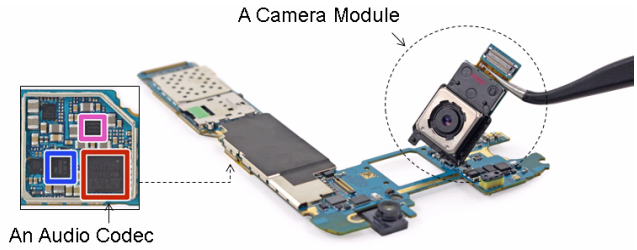

Fig. 1. Multimedia components integrated in a mobile device.

electromagnetic interference inside the device to improve the radio-frequency sensitivity [3, 4]. With the suppressed noise emissions, long-range noise detection of multimedia components becomes significantly challenging, and near-field noise measurement technologies have been exploited for component noise detection [5, 6]. Magnetic field probes have focused on near-field noise measurement owing to the gentle design flexibility and high sensitivity to printed circuit board–based systems [7]. However, the explicit relationship between near-field noise sources and magnetic field probes has not been introduced.

In this paper, an equivalent circuit model and an

analytic formula for near-field noise emissions are proposed to monitor multimedia operations in mobile devices. The proposed model includes a magnetic field probe and a transfer function for near-field magnetic coupling from a transmission line, which carries a current noise source to the magnetic field probe. With the proposed model, a magnetic field probe was optimally designed for noise measurement in a camera module and an audio codec integrated in a mobile device. It was successfully demonstrated that the probe captured the near-field noise emissions from 10 kHz to 100 MHz, depending on the operation conditions of the multimedia components, with enhanced sensitivity to a conventional reference probe.

2. Magnetic Field Probe Modeling

In order to estimate near-field noise emissions, an equivalent circuit model for a probe should be developed in advance. In this work, magnetic field probes were employed in consideration of the design flexibility and the high-sensitivity of the probes. Magnetic field probes are typically formed of single- or multiple-turn loops, on which currents are induced by time-variant magnetic fields penetrating the loop based on electromagnetic induction. Fig. 2(a) shows the design parameters of a magnetic probe, where N is the number of loop turns, and D and d are the diameters of the loops and the wire, respectively. Assuming that the probe is formed in air and does not contain magnetic materials, the inductance of the probe, L_p, is given by

$$L_p = N^2 \mu_0 \left(\frac{D}{2}\right)\left\{\ln\left(\frac{8D}{d}\right) - 2\right\} \text{ [H]} \quad (1)$$

where μ_0 is the permeability constant [8]. In ideal cases, a magnetic field probe is only characterized by inductance; however, the parasitic capacitance between the loops, C_p, and the series resistance of the wires, R_p, should be included in the model to improve the accuracy in a high-frequency range. For the parasitic capacitance and resistance calculation, Medhurst's formula and the skin effect frequency-dependent resistance model are employed as follows:

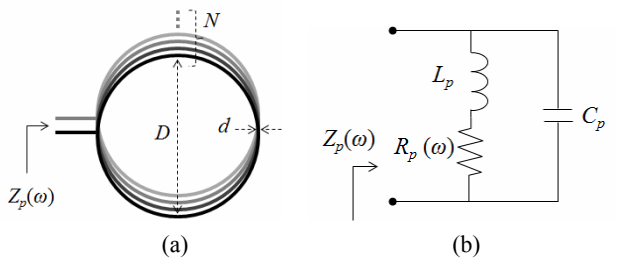

Fig. 2. (a) Design parameters of a magnetic field probe, (b) an equivalent circuit model.

$$C_p = \frac{4\varepsilon_0}{\pi}\left\{1 + 0.8249\left(\frac{D}{l}\right) + 2.329\left(\frac{D}{l}\right)^{3/2}\right\} \cdot l \text{ [F]} \quad (2)$$

$$R_p(\omega) = \rho\left(\frac{1}{\pi d^2} + \frac{1}{\pi d}\sqrt{\frac{\omega\mu_0}{\rho}}\right) \cdot l \text{ [}\Omega\text{]} \quad (3)$$

where l and ρ are the total length and the resistivity of the wire, and ε_0 is the permittivity constant [9, 10]. The total probe impedance can be derived by the combination of the circuit models, as shown in (4):

$$Z_p(\omega) = \left\{j\omega L_p + R_p(\omega)\right\} \| \left\{1/\left(j\omega C_p\right)\right\} \text{ [}\Omega\text{]} \quad (4)$$

To validate the probe model, impedance measurements were conducted using a vector network analyzer with magnetic field probes fabricated depending on design parameters. Fig. 3 shows the measured and modeled probe impedances, shown with solid and dotted lines, respectively, depending on the number of loop turns, N, where D and d are fixed at 26 mm and 0.5 mm. From 10 kHz to 500 MHz, it was demonstrated that the probe models agree with the measurement results. When N increases, the probe inductance and capacitance increase, resulting in shifting the resonance frequencies down. The resonance frequencies determine the probe bandwidth, in which magnetic field probes are valid.

3. Proposed Near-field Noise-emission Model and Experimental Verification

With the probe components modeled in the previous section, an equivalent circuit model for near-field noise emissions has been proposed. When a multimedia component is active in a mobile device, the components are synchronized with an operating clock, which propagate through transmission lines and generate significant near-field emissions via the transmission lines, which is a good antenna structure in terms of electromagnetic radiation.

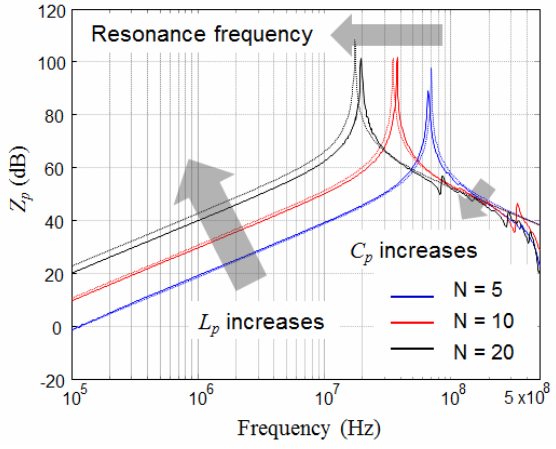

Fig. 3. Measured and modeled probe impedances depending on the number of loop turns, N (D=26mm, d=0.5mm).

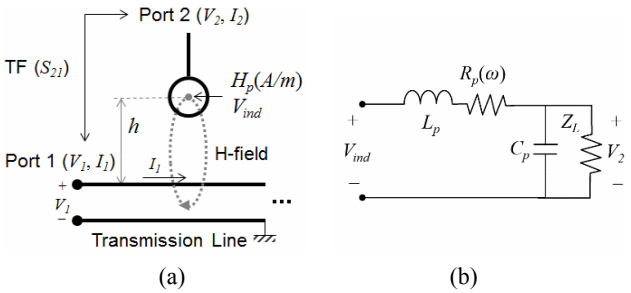

Fig. 4. (a) Near-field noise coupling from a transmission line to a magnetic field probe, (b) an equivalent circuit model.

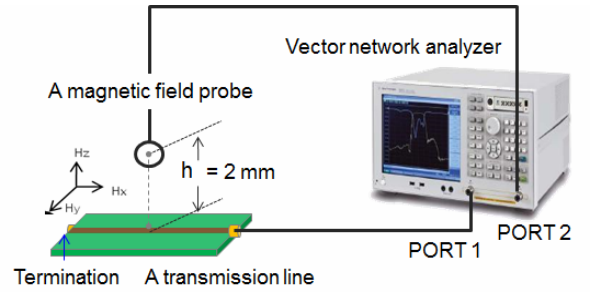

Fig. 5. Transfer function measurement setup.

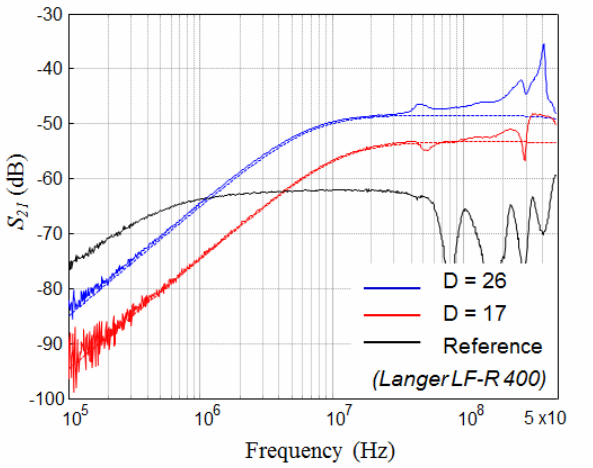

Fig. 6. Measured and modeled transfer functions depending on loop diameter D (N=5, d=0.5mm).

Fig. 4(a) shows the topology of near-field noise coupling from a transmission line to a magnetic field probe. The transmission line carries the noise current, I_1, injected from port 1 generating the magnetic field emission. The magnetic field, H_p, is captured by the magnetic field probe, inducing voltage V_{ind} at the probe loops. The magnetic field and the induced voltage in the probe are given by

$$H_p = I_1 / (2\pi h) \ \text{[A/m]} \tag{5}$$

$$V_{ind} = \omega \mu_0 H_p NA = \frac{\omega \mu_0 NAI_1}{2\pi h} \ \text{[V]} \tag{6}$$

where h is the probing height, and A is the loop area, which is πD^2 [11]. Fig. 4(b) depicts an equivalent circuit model for near-field coupling with a magnetic field probe. Associated with the equivalent circuit model, the voltage at port 2, V_2, and the transfer impedance, Z_{21}, can be obtained from the induced voltage at the probe, as shown in (7) and (8), respectively, where Z_L is the load impedance of the equipment, which is 50 Ohms.

$$V_2 = V_{ind} \left[\frac{1/(j\omega C_p)}{R_p(\omega) + j\omega L_p + 1/(j\omega C_p)} \right] \ \text{[V]} \tag{7}$$

$$Z_{21} = \left. \frac{V_2}{I_1} \right|_{I_2=0} = \frac{\omega \mu_0 NA}{2\pi h} \left[\frac{1/(j\omega C_p)}{R_p(\omega) + j\omega L_p + 1/(j\omega C_p)} \right] \ [\Omega] \tag{8}$$

The voltage transfer function, S_{21}, can be obtained from Z-parameters based on network parameter conversion (9) [12]. With the reciprocity theorem of Z-parameters, the transfer function can be simplified to (10) and represents the proposed near-field emission model, where Z_{22} is the probe impedance, Z_p.

$$S_{21} = \frac{2Z_{21}Z_0}{(Z_{11} + Z_0)(Z_{22} + Z_0) - Z_{12}Z_{21}} \tag{9}$$

$$S_{21} \approx \frac{2Z_{21}Z_0}{2Z_0(Z_p + Z_0) - Z_{21}^2} \tag{10}$$

To validate the proposed model, transfer function measurements were conducted with the measurement setup shown in Fig. 5. Port 1 of a vector network analyzer was connected to one end of a transmission line for excitation, and the other end was terminated to avoid multiple reflections. A magnetic probe was located 2 mm above the transmission line and was connected to port 2 to acquire the near-field noise emissions from the transmission line. Fig. 6 shows the measured and modeled transfer functions, shown with solid and dotted lines, respectively, depending on loop diameter D where N and d are fixed at 5 mm and 0.5 mm. The proposed near-field emission model was successfully demonstrated, with good agreement between the proposed models and the measurement results. With the proposed model, near-field noise coupling from the noise source to the magnetic field probe can be estimated, depending on the probe design. From the estimated noise emission characteristics, an optimal probe design can be obtained to achieve maximum sensitivity in a frequency range of the noise spectrum.

4. Near-field Noise Measurement of a Mobile Device

As an application of the proposed near-field noise emission model, noise spectrum measurements on a mobile device were conducted, and the measurement setup is shown in Fig. 7(a). The device under test (DUT) chosen

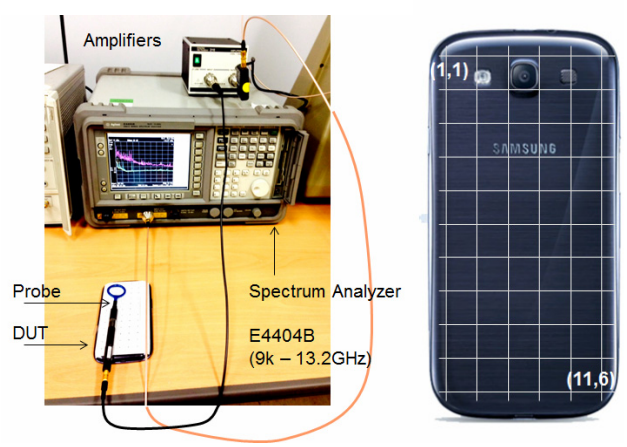

(a) (b)

Fig. 7. (a) Near-field noise measurement setup, (b) a mobile device as a device under test (DUT).

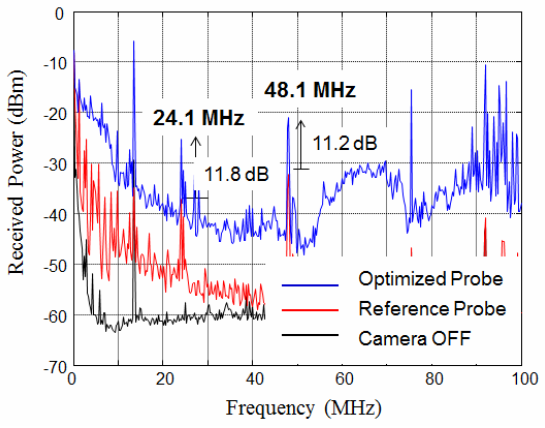

(a)

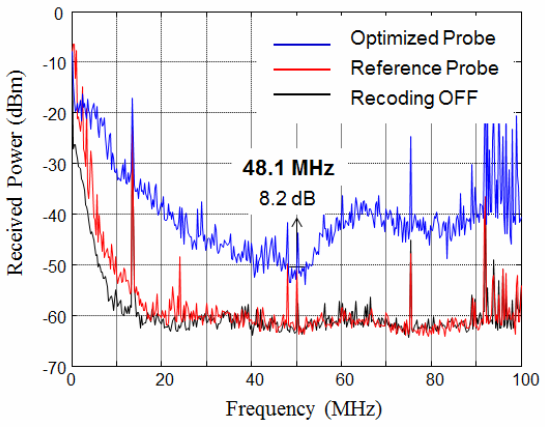

(b)

Fig. 8. Measured near-field noise spectrums depending on (a) camera operation, (b) recording operation.

was a smart phone that integrates a camera module and an audio codec component for entertainment purposes. With the proposed noise emission model, a near-field probe was optimally designed to capture the near-field emissions of a camera module and an audio codec with operating clock speeds of 24/48 MHz and 48 MHz only, respectively. To specify the locations of the components, two-dimensional coordinates are assigned on the DUT, as shown in Fig. 7(b). The camera module and the audio codec component are located at (3,2) and (9,1), respectively. The near-field probe was positioned at each location to capture the near-field emissions from the components. The captured noise emissions were amplified with a gain of 52 dB and were transferred to a spectrum analyzer. The noise spectrum measurements were carried out in the 100 kHz to 100 MHz frequency range and a max-hold acquisition.

Fig. 8 shows the spectrum measurement results of the near-field noise emissions from the camera module and the audio codec component, depending on the operating conditions. The lines in black represent the ambient noise spectrum measured by the reference probe with the multimedia components turned off. When the components are on and active, the captured noise increases at the operating clock frequencies. The measured noise spectrums with the optimized probe design in the proposed model, shown in blue, represent a significantly improved measurement sensitivity by around 10 dB compared to those with a conventional reference probe, shown in red. As for the noise characteristics, proper shielding techniques can be applied to achieve an improved signal-to-noise ratio (SNR), which was not applied to the probes fabricated for validation, but that should be considered in future works.

5. Conclusion

In this paper, we proposed an equivalent circuit model to detect near-field noise emissions from a magnetic field noise source. The transfer functions for near-field coupling from a transmission line to a magnetic field probe were extracted with the proposed model, and were experimentally verified with measurements. Based on the proposed model, an optimal probe design can be obtained to achieve maximum sensitivity in a frequency range of the noise spectrum. With a near-field probe optimally designed using the proposed model, it was successfully demonstrated that the probe achieved significantly enhanced sensitivity in noise spectrum measurement in a camera module with an audio codec in a mobile device. With the enhanced sensitivity in near-field measurement, the multimedia components can be monitored precisely, depending on the operating conditions.

Acknowledgement

The present research has been conducted by the research grant of National Security Research Institute in South Korea and Kwangwoon University in 2015.

References

[1] E. Magli and P. Frossard, “An overview of network coding for multimedia streaming,” *in Proc. IEEE Int. Conf. Multimedia and Expo., New York*, Jul. 2009, pp.

1488–1491. Article (CrossRef Link)
[2] M. Roessler, *How to find hidde cameras*, http://www.tentacle.franken.de/papers/hiddencams.pdf Article (CrossRef Link)
[3] T. Clupper, "Improve PCB shielding for portable devices," *Microw. RF*, 2003, 5, pp. 72–84. Article (CrossRef Link)
[4] G. Fenical, and P. Crotty, "Technology advancements in board level shields for EMI mitigation: not your daddy's metal can," *Compliance Mag.*, 2012, 7, pp. 24–31. Article (CrossRef Link)
[5] D. Baudry, C. Arcambal, A. Louis, B. Mazari and P. Eudeline, "Applications of the near-field techniques in EMC investigations," *IEEE Trans. Electromagn. Compat.*, vol. 49, no. 3, pp. 485–493, Aug. 2007. Article (CrossRef Link)
[6] S. Jarrix, T. Dubois, R. Adam, P. Nouvel, B. Azais and D. Gasquet, "Probe characterization for electromagnetic near-field studies," *IEEE Trans. Instrum. Meas.*, vol. 59, no. 2, pp. 292–300, Feb. 2010. Article (CrossRef Link)
[7] H. Chuang, G.-H. Li, E. Song, H. H. Park, H.-T. Jang, H. B. Park, Y.-J. Zhao, D. Pommerenke, T.-L. Wu and J. Fan, "A Magnetic-Field Resonant Probe With Enhanced Sensitivity for RF Interference Applications," *IEEE Trans. Electromagn. Compat.*, Vol. 55, No. 6, pp. 991-998, Dec. 10, 2013. Article (CrossRef Link)
[8] R. Lundin, "A Handbook Formula for the Inductance of a Single-Layer Circular Coil," *Proc. IEEE*, vol. 73, no. 9, pp. 1428-1429, Sep. 1985. Article (CrossRef Link)
[9] R. G. Medhurst, "H. F. resistance and self-capacitance of single-layer solenoids," *Wireless Eng.*, vol. 24, pp. 35–43, Feb. 1947 and pp. 80–92, Mar. 1946. Article (CrossRef Link)
[10] E. Bogatin, Signal Integrity—*Simplified. Englewood Cliffs, NJ: Prentice Hall*, 2004. Article (CrossRef Link)
[11] X. Dong, S. Deng, T. Hubing and D. Beetner, "Analysis of Chip-level EMI using Near-Field Magnetic Scanning," *IEEE Int. Symposium on Electromagnetic Compatibility*, pp.174-177, Aug. 2004. Article (CrossRef Link)
[12] D. M. Pozar, *Microwave Engineering 3rd*. John Wiley & Sons, Inc. 2005. Article (CrossRef Link)

Eakhwan Song received the B.S., M.S., and Ph.D. degrees in electrical engineering from the Korea Advanced Institute of Science and Technology (KAIST), Daejeon, Korea, in 2004, 2006, and 2010, respectively. In 2008, he was a Technical Co-op. in the IBM Systems and Technology Group (STG), Poughkeepsie, NY, USA, where he was the recipient of the Best Hardware Award in IBM Early Tenure TechConnect 2008. In 2010, he was a Postdoctoral Researcher at KAIST, where he was engaged in high-speed signal integrity and power integrity design in system-in-package, and equalizer design in high-speed serial links. From 2011 to 2013, he was with the Global Technology Center (GTC), Samsung Electronics, as a Senior Engineer. In Samsung Electronics, he worked focusing on high-speed serial interconnects design and electromagnetic compatibility/ interference (EMC/EMI) design for ICs, packages, and highly-integrated mobile devices. He is currently an Assistant Professor with the Department of Electronics and Communication Engineering in Kwangwoon University, Seoul, South Korea, since 2014. His research interests include system-level EMC/EMI, multigigabit serial interface design, and advanced electromagnetic applications.

Jieun Choi received the B.S degree in electrical engineering from the KOREA university, Seoul, Korea, in 2007 and M.S. degree in electrical engineering from the Korea Advanced Institute of Science and Technology (KAIST), Daejeon, Korea, in 2009. She is currently researcher in National Security Research Institute (NSR).

Young-Jun Lee received the B.S., M.S., and Ph.D. degrees in electronics engineering from Pusan National University (PNU), Busan, Korea, in 2006, 2008 and 2012, respectively. He is currently working at National Security Research Institute (NSR), Daejeon, Korea. His main research interests are in the area of digital signal processing, adaptive filtering, array signal processing, in particular signal processing for digital broadcasting and communication systems.